

New Suns in the Cosmos II: Differential rotation in *Kepler* Sun-like stars

M. L. Das Chagas^{1,2}, J. P. Bravo¹, A. D. Costa¹, C. E. Ferreira Lopes⁶,
R. Silva Sobrinho¹, F. Paz-Chinchón^{7,8}, I. C. Leão³, A. Valio⁵, D. B. de Freitas¹,
B. L. Canto Martins¹, A. F. Lanza⁴ and J. R. De Medeiros¹

¹*Departamento de Física Teórica e Experimental, Universidade Federal do Rio Grande do Norte, Natal, RN 59078-970, Brazil*

²*Faculdade de Física - Instituto de Ciências Exatas, Universidade Federal do Sul e Sudeste do Pará, Marabá, PA 68505-080, Brazil*

³*European Southern Observatory, Karl-Schwarzschild-Strasse 2, Garching 85748, Germany*

⁴*INAF, Osservatorio Astrofisico di Catania, via S. Sofia, 78, Catania 95123, Italy*

⁵*CRAAM, Universidade Presbiteriana Mackenzie, Rua da Consolação, 896, São Paulo, SP 01302, Brazil*

⁶*SUPA Wide-Field Astronomy Unit, Institute for Astronomy, School of Physics and Astronomy, University of Edinburgh, Royal Observatory, Blackford Hill, Edinburgh EH9 3HJ, UK*

⁷*Departamento de Enseñanza de las Ciencias Básicas, Universidad Católica del Norte, Larrondo 1281, Coquimbo 17814-21, Chile*

⁸*Millennium Institute of Astrophysics, Av. Vicuña Mackenna 4860, Macul, Santiago 78204-36, Chile*

Accepted 2016 August 10. Received 2016 August 8; in original form 2016 April 5

ABSTRACT

The present study reports the discovery of Sun-like stars, namely main-sequence stars with T_{eff} , $\log g$ and rotation periods P_{rot} similar to solar values, presenting evidence of surface differential rotation. An autocorrelation of the time series was used to select stars presenting photometric signal stability from a sample of 881 stars with light curves collected by the *Kepler* space-borne telescope, in which we have identified 17 stars with stable signals. A simple two-spot model together with a Bayesian information criterion were applied to these stars in the search for indications of differential rotation; in addition, for all 17 stars, it was possible to compute the spot rotation period P , the mean values of the individual spot rotation periods and their respective colatitudes, and the relative amplitude of the differential rotation.

Key words: stars: rotation, (stars:) starspots, stars: solar-type

1 INTRODUCTION

Stars are normally born with rapid rotation, and the angular velocity distribution will be established in their infancy stages, mostly as the result of the interaction of the stellar magnetic field with the circumstellar accretion disk, at least for late-type stars (e.g., Shu et al. 1994; Bouvier et al. 1997; van Saders & Pinsonneault 2013). During the initial stages, the surfaces of stars with convective envelopes will slow down via magnetic braking resulting from the interaction between the stellar magnetic field and the magnetized wind from the surface (e.g., Kawaler 1988; Reiners & Mohanty 2012).

Surface rotation can now be measured for many families of stars using different procedures, including the analyses of spectral line broadening, which pro-

duces projected rotational velocity $v \sin(i)$ measurements (e.g., De Medeiros & Udry 1999; De Medeiros et al. 2014; Nordström et al. 2004), and periodic modulation of starlight produced by non-uniformities on the surface of the stars (e.g., Affer et al. 2012; De Medeiros et al. 2013; McQuillan et al. 2014; Leão et al. 2015). Other procedures include those based on line core variations in the Ca II H and K lines (e.g., Baliunas et al. 1983) and on the Rossiter-McLaughlin effect or ellipsoidal light variations in eclipsing binaries.

In addition, it is now well established that the surface and internal stellar rotation pattern is by no means uniform. For instance, Helioseismology has revealed a large spread of rotation rates in the outer convective regions at different latitudes, with the inner regions presenting an almost constant rotation rate (e.g., Aerts et al. 2010). These aspects are in-

timately associated with the stellar differential rotation (hereafter DR), i.e., the property that different parts of the star rotate at different rates (Miesch 2005; Miesch & Toomre 2009; Kitchatinov 2013). The current leading theoretical basis, first presented by Ledinsky (1941), explains differential rotation based on the interaction between convection and rotation, with convective motions in a rotating star being disturbed by the Coriolis force. Its back reaction redistributes angular momentum and disturbs the global rotation behavior to produce non-uniformities, leading to DR of the surface.

Different procedures can be used in the diagnosis of surface DR. In the first procedure, Doppler imaging, the positions of individual spots are estimated based on their effects on the stellar spectral line profiles, on the condition that the star is rotating rapidly enough (e.g., Collier Cameron et al. 2002). In the second procedure, the Fourier transform method, the Doppler shift at different latitudes due to rotation can be estimated from the Fourier transform of the line profiles (e.g., Reiners & Schmitt 2003; Reinhold & Reiners 2013). In the third procedure, time series photometry, the rotation periods can be computed from a time series of photometric observations (e.g., Aigrain et al. 2015; Lanza et al. 2014; Davenport et al. 2015). Another approach is based on Asteroseismology, in which the frequency splitting of global oscillations is explained in terms of different latitudinal rotation rates (e.g., Gizon & Solanki 2004). A recent blind survey of competing techniques for detecting rotation and DR from model photometry, conducted by Aigrain et al. (2015), showed excellent agreement in recovering the overall rotation periods for stars exhibiting low and moderate activity levels. However, the referred study revealed a complex degeneracy between DR shear, spot lifetimes, and the number of spots present, suggesting that DR studies based on full-disc light curves alone need to be treated with caution.

The advent of the space-borne CoRoT (Baglin et al. 2006) and *Kepler* (Borucki et al. 2010) telescopes made it possible to study in great detail the behavior of the rotation of Sun-like stars. In this context, a large effort is being directed at the analysis of more active stars using the photometric modulations observed from their light curve (e.g., Fröhlich et al. 2012; Bonomo & Lanza 2012; McQuillan et al. 2013; De Medeiros et al. 2013), therein producing rotation periods for thousands of different families of stars. A parallel effort is being made by different authors to enlarge the horizons of our quantitative and qualitative understanding of DR (e.g., Reinhold et al. 2013; Reinhold & Reiners 2013; Lanza et al. 2014; Aigrain et al. 2015; Reinhold & Gizon 2015).

Most of the DR surface patterns observed to date are predominantly solar-type, with rotation rates decreasing from the equatorial to polar regions (e.g., Reinhold & Reiners 2013; Lanza et al. 2014; Collier Cameron et al. 2002; Reiners & Schmitt 2003; Lanza et al. 1993; Baliunas et al. 1983). The DR total sur-

face gradient varies to a high degree with the effective temperature (Barnes et al. 2005) and to a low degree with the rotation rate (Küker & Rüdiger 2005). Antisolar DR measurements are sparse and have mainly been performed for some late-type giant stars, most of which being components of RS CVn-systems (e.g., Strassmeier et al. 2003; Oláh et al. 2003; Weber et al. 2005; Vida et al. 2007). As noted by different authors (e.g., Kovári et al. 2015), it appears that the strength and even the orientation of the DR are influenced by close companions, although such a scenario is not yet understood.

By applying asteroseismology procedures to time series obtained from light curve (hereafter LC) data from the *Kepler* or CoRoT missions, we are now in a position to extract, in addition to information about the surface rotational pattern, the physical characteristics of the stellar interior, revealing not only relevant aspects of DR but also information about pulsation modes and important constraints for dynamo models of low-mass stars. This enables one to test theoretical models for internal DR (see, e.g., Kitchatinov & Olemskoy 2011; Küker & Rüdiger 2011a), as well as the development of 3D simulations (e.g., Brun 2004; Browning 2008; Käpylä et al. 2012). Further, it has been possible to estimate the ratio between the rotation rate in the small helium core and the large convective regions of late-type stars (e.g., Eggenberger et al. 2010).

This is the 2nd paper of a series of studies devoted to the identification of Sun-like stars presenting physical properties similar to the Sun. In the 1st study (De Freitas et al. 2013), we identified stars representing potentially good matches to the Sun’s rotation. The main goal of the present work is to apply spot modeling (Lanza et al. 2014) for a large sample of Sun-like stars observed in the scope of the *Kepler* mission, therein attempting to measure DR and quantify how common DR is among Sun-like stars presenting solar parameters and, in particular, stars with similar Sun rotation periods.

This paper is organized as follows: Section 2 presents the stellar sample with the *Kepler* stellar parameters. In Section 3, we introduce the autocorrelation function. Results and Conclusions are presented in Sections 4 and 5, respectively.

2 WORKING SAMPLE AND DATA ANALYSES

From May 2009 to May 2013, the *Kepler* mission collected data in a steady field of view for 191,449 stars in 17 runs (known as quarters), which were composed of long-cadence (6.02 s observations stacked every 29.4 minutes, (Jenkins et al. 2010)) and short-cadence (bins of 59 s) observations (Van Cleve et al. 2010; Thompson et al. 2013). For the present study, we selected the calibrated LCs processed by the PDC-MAP pipeline (Jenkins et al. 2010). To search for stars with physical properties approximately equal to the solar values, we made an initial selection of LCs

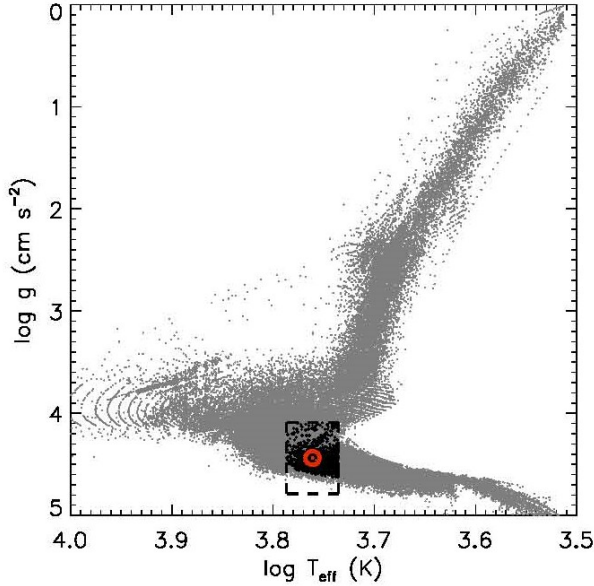


Figure 1. Distribution of $\log g$ and T_{eff} from entire *Kepler* database. The black rectangle denotes the region of sources with solar parameters with T_{eff}^{\odot} and $\log g^{\odot}$. The red circle shows the position of the Sun, and the small cross is the sample analysed.

from the *Kepler* database (Mikulski Archive for Space Telescopes¹) using the solar parameters $\log g$ (~ 4.44) cm s^{-2} , T_{eff} (~ 5779) K, $[Fe/H]$ ($\sim 0.$) dex and 23 days $< P_{\text{rot}} < 33$ days. A total of 881 stars with 3.94 $\text{cm s}^{-2} < \log g < 4.94$ cm s^{-2} , 5579 K $< T_{\text{eff}} < 5979$ K, were selected, with effective temperature and gravity obtained from Huber et al. (2014) and rotation period given by McQuillan et al. (2013). The location of our working sample, in the $\log g$ versus T_{eff} diagram, in the context of the entire *Kepler* stellar sample, is displayed in Fig. 1. With such a working sample at hand, a careful treatment was applied to the LCs, using the so-called co-trending basis vectors provided by the *Kepler* archive (see Smith et al. 2012; Stumpe et al. 2012; Twicken et al. 2010), to remove systematic long-term trends originating from instruments, the environment, the detector, or effects caused by the re-orientation of the spacecraft after each ~ 90 days. To remove outliers and prepare the LCs for the analysis using spot modelling, we applied the method developed by De Medeiros et al. (2013), a procedure that is able to identify discontinuities in the LCs, similar to that used by Basri et al. (2011). From this point on, an LC was considered to be fully treated, and its spot modelling analysis could be performed.

¹ http://archive.stsci.edu/kepler/data_search/search.php, hereafter MAST

3 THE AUTOCORRELATION METHOD

In this work, we follow the same procedure developed by Lanza et al. 2014 to estimate surface DR. First, we applied an autocorrelation function (ACF) to check the stability of the photometric signal. Indeed, an important feature of the ACF is that it exhibits an oscillatory behavior with regularly spaced peaks; then, the coherence of a photometric signal can be estimated by the relative height of successive peaks in the ACF (Lanza et al. 2014). A crucial step in our analysis was the search for photometric signal stability for all 881 LCs constituting our initial working sample. From such analyses, we identified 17 stars presenting unambiguous stable photometric signals, indicating rotational modulation. Nevertheless, in spite of the fact that a significant DR can be detected when the relative height of the second maximum in the ACF is at least 0.6-0.7 (Lanza et al. 2014), we have considered a few stars whose ACF has a peak ratio small than this threshold because the Monte Carlo Markov chain (MCMC) analysis points for a significant DR for them. These stars with less good ACFs are flagged by a dagger in Table 2. Indeed, the ACF has been widely used in the study of photometric signals due to its ability to provide a good estimate of the average period variability, including stellar rotation period (e.g., McQuillan et al. 2013; Affer et al. 2012). Then, for these 17 stars with sufficiently stable signals, we applied spot modelling (Lanza et al. 2014) to seek individual spot rotation periods. The method of spot modelling is based on two spots and was applied with a Bayesian information criterion (hereafter BIC) to initially choose intervals of the time series presenting evidence of differential rotation with starspots of almost constant areas. The initial and final times t_1 and t_2 , respectively, of those intervals are given in Table 1, together with the BIC computed values for each of the 17 stars. Indeed, t_1 and t_2 are defined in Barycentric Kepler Julian Day (BKJD). Even if the time intervals are particularly small, the spot modelling is able to give us a valid signal of DR, as many other authors (e.g., Croll et al. 2006; Fröhlich 2007) have proven in previous studies. Readers are referred to Lanza et al. (2014) for a complete discussion of the ACF and the spot modelling procedure. Nevertheless, let us underline an important aspect, previously considered by different authors (e.g., Davenport et al. 2015; Jeffers & Keller 2009), in the context of the present procedure. In the applied two-spot modelling, we cannot constrain the total number of starspots on the stellar surface, which, as noted by Davenport et al. (2015), may reflect two groups of spots or even many small spots across the entire stellar surface.

The LCs and the oscillatory behaviour of the ACF for these 17 stars are shown in Fig. A1 of Appendix A. The blue vertical solid lines display the initial and final times t_1 and t_2 of the intervals considered for the MCMC analysis. We then applied the procedure by Lanza et al. (2014) to compute the spot rotation period P , the mean values of the individual spot rotation periods P_1 and P_2 and their respective

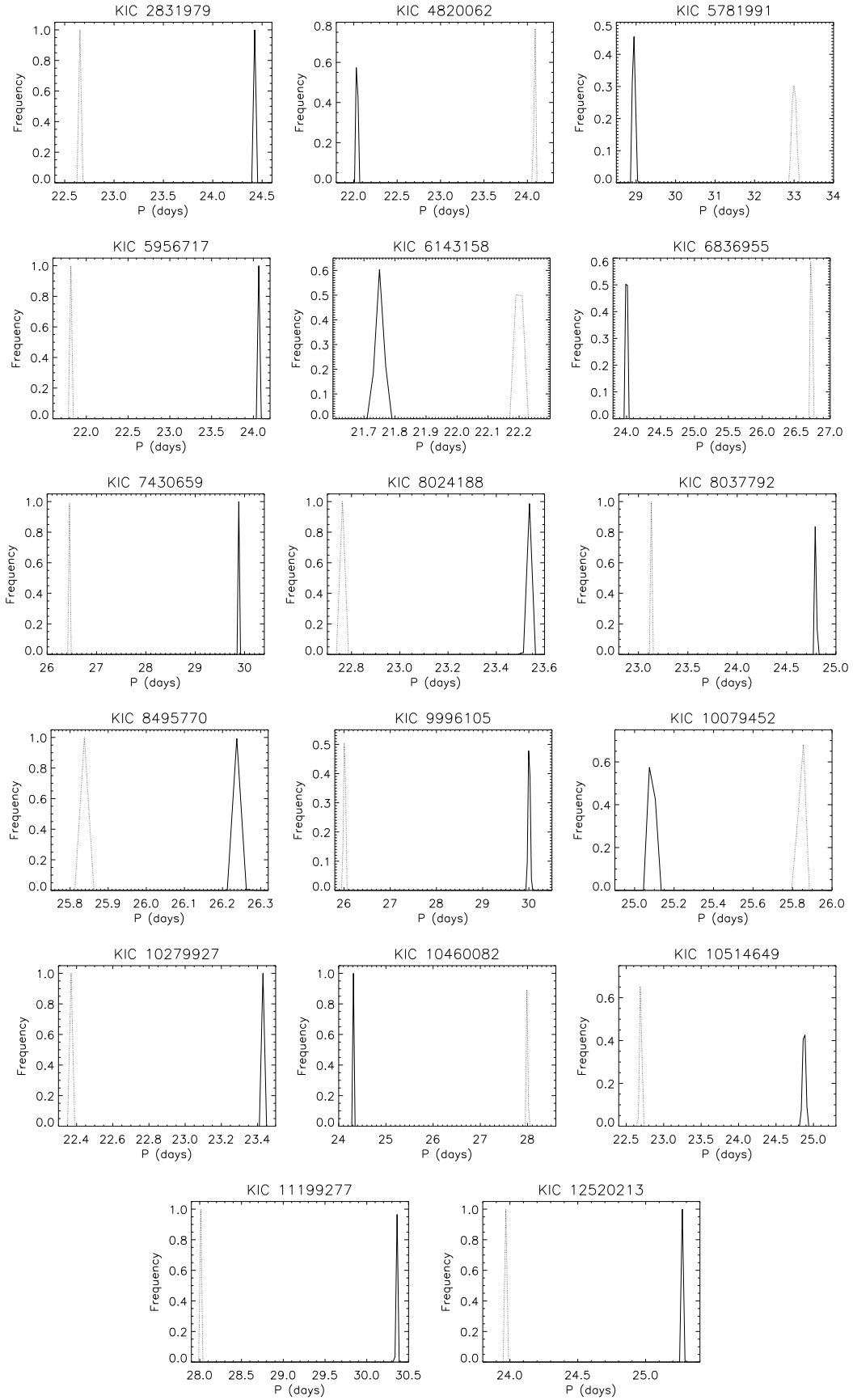


Figure 2. A posteriori distributions of the rotation periods of the two spots as derived from MCMC for all stars. The solid line refers to the distribution of the rotation period of the first spot, and the dashed line refers to that of the second.

Table 1. Initial and final times of the intervals considered for the MCMC analysis, together with the BIC computed values.

Star (KIC #)	t_1 (BKJD)	t_2 (BKJD)	BIC
2831979	1212.163	1255.382	4.097
4820062	735.384	761.804	18.778
5781991	131.513	164.984	5.300
5956717	1182.758	1207.585	8.027
6143158	411.224	439.158	17.008
6836955	261.205	293.591	10.65
7430659	863.035	899.592	3.261
8024188	1201.311	1240.893	7.467
8037792	634.978	676.926	16.325
8495770	844.746	880.383	19.635
9996105	264.290	336.132	3.183
10079452	448.517	499.623	8.413
10279927	1216.781	1239.504	18.279
10460082	416.803	442.203	11.926
10514649	205.096	247.352	4.528
11199277	1419.912	1465.927	14.378
12520213	820.143	869.328	7.102

colatitudes, θ_1 and θ_2 , and the relative amplitude of the DR, $\Delta P/P$, where $P = (P_1 + P_2)/2$. The a posteriori distributions of the rotation periods P_1 and P_2 of the two spots for all 17 stars, as derived from MCMC, are given in Fig. 2. The standard deviations of $\Delta P/P$ were also estimated by a model that assumes that starspots are not evolving along the fitted interval. Starspot evolution can limit our accuracy in measuring differential rotation at $\Delta\Omega \sim 1/t_{\text{evol}}$, where t_{evol} is the evolutionary timescale, or even mimic a differential rotation signal in the worst cases (see Aigrain et al. 2015).

4 RESULTS

The main results of the present study are given in Table 2, which lists the mean values of the individual spot rotation periods P_1 and P_2 , the relative amplitude of the DR lower limit, $\Delta P/P$ and the amplitude of the DR expressed as the frequency difference between the spots frequencies, $\Delta\Omega$. Table 2 lists also the stellar parameters P_{rot} , $\log g$ and T_{eff} . Fig. 3 displays, in the $\log g$ vs. T_{eff} diagram, the locations of the 881 stars defined in our selection criteria, namely stars showing physical properties that are approximately equal to the Sun values, with $3.94 \text{ cm s}^{-2} < \log g < 4.94 \text{ cm s}^{-2}$, $5579 \text{ K} < T_{\text{eff}} < 5979 \text{ K}$, and the rotation period ranging into the solar values, from 23 days $< P_{\text{rot}} < 33$ days. In the referred figure, the red points represent the 17 stars having spot lifetimes long enough for the detection of DR patterns on the basis of our spot modelling method. Evolutionary tracks taken from Ekström et al. (2012) are overlaid to constrain the view of the mass range and evolutionary stage of the sample stars, with the position of the Sun indicated by the black symbol.

We compared the present results with Reinhold

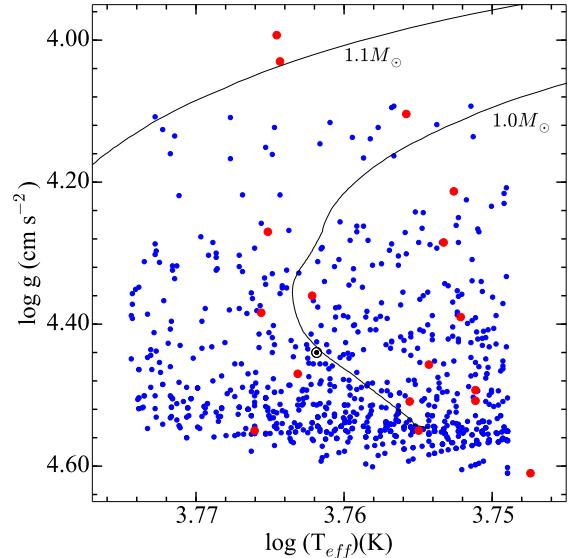


Figure 3. Distribution of Sun-like stars with measured DR in the $\log g$ and T_{eff} diagram, represented by red circles. Blue circles indicate stars of the original working sample without traces of DR. The evolutionary tracks are from Ekström et al. (2012).

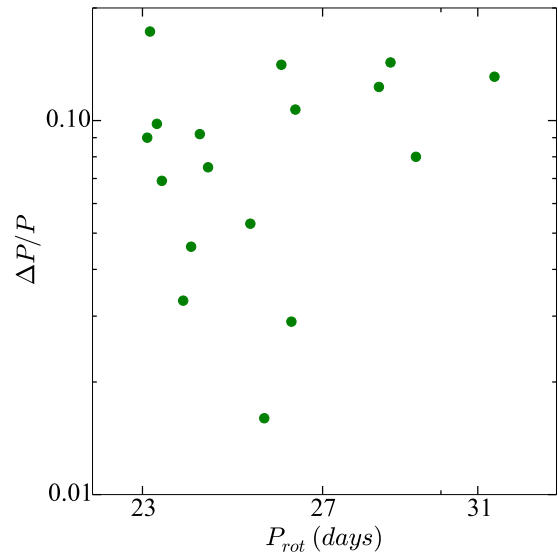


Figure 4. The distribution of the relative amplitude $\Delta P/P$ versus the rotation period P_{rot} for the 17 Sun-like stars with DR traces identified in the present study.

& Gizon (2015). Indeed, from our sample of 17 stars with measured amplitude of surface DR, 11 stars are found to be in common with those authors. For these common stars, Reinhold & Gizon (2015) detected the presence of multiple periods in their LCs, which were interpreted as the manifestation of DR, using a different approach based on the Lomb-Scargle periodogram. These stars are identified in Table 2 with an asterisk. A simple comparison between the DR values of this small sample of targets in common

Table 2. The stellar parameters and the results of MCMC analysis for our sample of 17 stars with traces of DR.

Star (KIC #)	P_{rot} (d)	$\log g$ (cm s^{-2})	T_{eff} (K)	P_1 (d)	σP_1 (d)	P_2 (d)	σP_2 (d)	$\Delta P/P$	$\sigma \Delta P/P$	$\Delta \Omega$ (d)
2831979*	24.383	4.363	5783	24.433	9.597×10^{-4}	22.660	1.629×10^{-3}	0.0753	8.332×10^{-5}	0.02012
4820062*	23.098	4.104	5699	22.634	1.296×10^{-3}	24.771	2.676×10^{-3}	0.0886	1.347×10^{-4}	0.02395
5781991†	31.464	4.466	5796	28.947	3.150×10^{-2}	33.006	4.909×10^{-2}	0.1310	2.007×10^{-3}	0.02669
5956717*	23.297	4.213	5657	24.069	9.727×10^{-4}	21.828	6.862×10^{-4}	0.0976	5.440×10^{-5}	0.02679
6143158†	23.155	4.509	5696	25.513	6.648×10^{-3}	21.448	2.218×10^{-3}	0.1731	3.243×10^{-4}	0.04667
6836955†	26.354	4.61	5590	24.000	9.132×10^{-3}	26.724	5.223×10^{-3}	0.1074	4.371×10^{-4}	0.02668
7430659*	28.388	4.268	5823	29.897	1.377×10^{-3}	26.440	2.351×10^{-3}	0.1227	1.027×10^{-4}	0.02748
8024188*	23.849	4.384	5829	23.528	1.587×10^{-3}	22.754	1.653×10^{-3}	0.0334	1.007×10^{-4}	0.00908
8037792*†	23.400	4.285	5666	24.797	3.245×10^{-3}	23.132	2.280×10^{-3}	0.0695	1.712×10^{-4}	0.01823
8495770*†	25.634	4.545	5688	26.244	2.802×10^{-3}	25.832	1.605×10^{-3}	0.0158	1.250×10^{-4}	0.00383
9996105	28.683	3.990	5815	30.006	1.936×10^{-2}	26.012	1.881×10^{-2}	0.1426	1.032×10^{-3}	0.03215
10079452*	26.261	4.030	5812	25.092	7.177×10^{-3}	25.842	3.767×10^{-3}	0.0294	3.230×10^{-4}	0.00726
10279927	24.018	4.508	5638	23.429	7.529×10^{-4}	22.373	8.778×10^{-4}	0.0461	5.166×10^{-5}	0.01265
10460082*	26.027	4.554	5835	24.321	2.090×10^{-3}	28.001	3.333×10^{-3}	0.1407	1.610×10^{-4}	0.03396
10514649*	24.205	4.388	5651	24.875	1.740×10^{-2}	22.694	1.084×10^{-2}	0.0917	9.016×10^{-4}	0.02428
11199277*	29.339	4.493	5638	30.356	3.538×10^{-3}	28.019	1.479×10^{-3}	0.0801	1.366×10^{-4}	0.01726
12520213	25.318	4.457	5679	25.270	3.361×10^{-3}	23.967	2.941×10^{-3}	0.0529	1.862×10^{-4}	0.01352

*Stars with manifestation of DR, which are in common with [Reinhold & Gizon \(2015\)](#).

†Stars with ACFs lower than the threshold 0.6-0.7.

provides no correlation between the values, although they are distributed in a similar range. As a more robust test, we applied Student's t-test, which can be used to compare whether measures in one sample are paired with measures in another sample. According to this method, the null hypothesis assumes that the true mean difference between the two observations on each sample is zero; otherwise, the alternative hypothesis is considered. In this sense, the results of the paired t-test show that, because the $-t_{0.025}(-2.228) < t_{\text{computed}}(-0.959) < t_{0.025}(2.228)$ and because the p-value > 0.05 (confidence level), we cannot reject the null hypothesis. Such a fact may reflect, in principle, the difference in the nature of the procedures applied in the search for DR traces. In addition, the compatibility between their ranges suggests that their information is valid at least up to an order of magnitude.

Finally, we analysed the behaviour of the relative amplitude $\Delta P/P$ as a function of rotation period for our sample of 17 stars despite the narrow range of rotation periods considered in the present study, namely, from 23 to 33 days. Fig. 4 displays the behaviour of P_{rot} vs. $\Delta P/P$, from which one observes a soft trend of increasing $\Delta P/P$ towards longer rotation periods, paralleling the scenario found by different studies. For instance, as shown by [Reinhold et al. \(2013\)](#), the relative DR shear increases with longer rotation periods, in agreement with previous observations ([Barnes et al. 2005](#)) and theoretical approaches ([Küker & Rüdiger 2011b](#)).

5 CONCLUSIONS

Based on a simple two-spot model together with a Bayesian information criterion, we measured a lower limit on the amplitude of surface DR for 17 *Kepler*

Sun-like stars. For these stars, using *Kepler* high-precision and evenly sampled photometric time series, it was possible to compute the spot rotation period P , the mean values of the individual spot rotation periods P_1 and P_2 and the relative amplitude of the differential rotation, $\Delta P/P$, where $P = (P_1 + P_2)/2$. These stars present a soft trend of the estimated relative amplitude, $\Delta P/P$, increasing with increasing rotation periods, in agreement with the scenarios found in the literature, from several observational studies of DR, based on different measurement approaches.

In summary, although the art of measurements of the surface rotation of stars has now been mastered, with a high level of precision and maturity, the detection and measurement of stellar differential rotation remains a tricky subject. In the present study, using a spot-modelling procedure, we were able to detect surface differential rotation patterns in 17 stars with physical properties, including rotation, similar to the Sun. The portrait emerging from the present study points to a significant perspective: among Sun-like stars with surface rotation similar to the solar values, surface differential rotation appears to be a common phenomenon.

ACKNOWLEDGEMENTS

The research activity of the Observational Astronomy Board of the Federal University of Rio Grande do Norte (UFRN) is supported by continuous grants from CNPq and FAPERN Brazilian agencies. We also acknowledge financial support from INCT Espaço/CNPq/MCT. MLC, JPB and ADC acknowledge CAPES/PNPD fellowships. ICL and CEFL acknowledge CNPq/PDE fellowships. RSB and FPC acknowledge graduate fellowships from CAPES. D. B de Freitas also acknowledges financial support by

the Brazilian agency CNPq (Grant No. 306007/2015-0). This paper includes data collected by the *Kepler* mission. Funding for the *Kepler* mission is provided by the NASA Science Mission directorate. All *Kepler* data presented in this paper were obtained from the Mikulski Archive for Space Telescopes (MAST). We would like to thank the anonymous referee for the helpful comments that lead us to a substantial improvement of this manuscript.

REFERENCES

- Aerts C., et al., 2010, *A&A*, **513**, L11
- Affer L., Micela G., Favata F., Flaccomio E., 2012, *MNRAS*, **424**, 11
- Aigrain S., et al., 2015, *MNRAS*, **450**, 3211
- Baglin A., Auvergne M., Barge P., Deleuil M., Catala C., Michel E., Weiss W., COROT Team 2006, in Fridlund M., Baglin A., Lochard J., Conroy L., eds, ESA Special Publication Vol. 1306, ESA Special Publication. p. 33
- Baliunas S. L., et al., 1983, *ApJ*, **275**, 752
- Barnes J. R., Collier Cameron A., Donati J.-F., James D. J., Marsden S. C., Petit P., 2005, *MNRAS*, **357**, L1
- Basri G., et al., 2011, *AJ*, **141**, 20
- Bonomo A. S., Lanza A. F., 2012, *A&A*, **547**, A37
- Borucki W. J., et al., 2010, *Science*, **327**, 977
- Bouvier J., Forestini M., Allain S., 1997, *A&A*, **326**, 1023
- Browning M. K., 2008, *ApJ*, **676**, 1262
- Brun A. S., 2004, in Danesy D., ed., ESA Special Publication Vol. 559, SOHO 14 Helio- and Asteroseismology: Towards a Golden Future. p. 271
- Collier Cameron A., Donati J.-F., Semel M., 2002, *MNRAS*, **330**, 699
- Croll B., et al., 2006, *ApJ*, **648**, 607
- Davenport J. R. A., Hebb L., Hawley S. L., 2015, *ApJ*, **806**, 212
- De Freitas D. B., Leão I. C., Ferreira Lopes C. E., Paz-Chinchon F., Canto Martins B. L., Alves S., De Medeiros J. R., Catelan M., 2013, *ApJ*, **773**, L18
- De Medeiros J. R., Udry S., 1999, *A&A*, **346**, 532
- De Medeiros J. R., et al., 2013, *A&A*, **555**, A63
- De Medeiros J. R., Alves S., Udry S., Andersen J., Nordström B., Mayor M., 2014, *A&A*, **561**, A126
- Eggenberger P., et al., 2010, *A&A*, **519**, A116
- Ekström S., et al., 2012, *A&A*, **537**, A146
- Fröhlich H.-E., 2007, *Astronomische Nachrichten*, **328**, 1037
- Fröhlich H.-E., Frasca A., Catanzaro G., Bonanno A., Corsaro E., Molenda-Žakowicz J., Klutsch A., Montes D., 2012, *A&A*, **543**, A146
- Gizon L., Solanki S. K., 2004, *Sol. Phys.*, **220**, 169
- Huber D., et al., 2014, *ApJS*, **211**, 2
- Jeffers S. V., Keller C. U., 2009, in Stempels E., ed., American Institute of Physics Conference Series Vol. 1094, 15th Cambridge Workshop on Cool Stars, Stellar Systems, and the Sun. pp 664–667, doi:10.1063/1.3099201
- Jenkins J. M., et al., 2010, *ApJ*, **713**, L87
- Käpylä P. J., Mantere M. J., Brandenburg A., 2012, *ApJ*, **755**, L22
- Kawaler S. D., 1988, *ApJ*, **333**, 236
- Kitchatinov L. L., 2013, in Kosovichev A. G., de Gouveia Dal Pino E., Yan Y., eds, IAU Symposium Vol. 294, IAU Symposium. pp 399–410 (arXiv:1210.7041), doi:10.1017/S1743921313002834
- Kitchatinov L. L., Olemskoy S. V., 2011, *MNRAS*, **411**, 1059
- Kovári Z., et al., 2015, *A&A*, **573**, A98
- Küker M., Rüdiger G., 2005, *Astronomische Nachrichten*, **326**, 265
- Küker M., Rüdiger G., 2011a, *Astronomische Nachrichten*, **332**, 83
- Küker M., Rüdiger G., 2011b, *Astronomische Nachrichten*, **332**, 933
- Lanza A. F., Rodono M., Zappala R. A., 1993, *A&A*, **269**, 351
- Lanza A. F., Das Chagas M. L., De Medeiros J. R., 2014, *A&A*, **564**, A50
- Leão I. C., et al., 2015, *A&A*, **582**, A85
- Lebedinsky A. I., 1941, *Astron. Zh*, **18**, 10
- McQuillan A., Aigrain S., Mazeh T., 2013, *MNRAS*, **432**, 1203
- McQuillan A., Mazeh T., Aigrain S., 2014, *ApJS*, **211**, 24
- Miesch M. S., 2005, *Living Reviews in Solar Physics*, **2**, 1
- Miesch M. S., Toomre J., 2009, *Annual Review of Fluid Mechanics*, **41**, 317
- Nordström B., et al., 2004, *A&A*, **418**, 989
- Oláh K., Jurcsik J., Strassmeier K. G., 2003, *A&A*, **410**, 685
- Reiners A., Mohanty S., 2012, *ApJ*, **746**, 43
- Reiners A., Schmitt J. H. M. M., 2003, *A&A*, **398**, 647
- Reinhold T., Gizon L., 2015, *A&A*, **583**, A65
- Reinhold T., Reiners A., 2013, *A&A*, **557**, A11
- Reinhold T., Reiners A., Basri G., 2013, *A&A*, **560**, A4
- Shu F., Najita J., Ostriker E., Wilkin F., Ruden S., Lizano S., 1994, *ApJ*, **429**, 781
- Smith J. C., et al., 2012, *PASP*, **124**, 1000
- Strassmeier K. G., Kratzwald L., Weber M., 2003, *A&A*, **408**, 1103
- Stumpe M. C., et al., 2012, *PASP*, **124**, 985
- Thompson M. A., et al., 2013, *PASP*, **125**, 809
- Twicken J. D., Chandrasekaran H., Jenkins J. M., Gunter J. P., Girouard F., Klaus T. C., 2010, in Society of Photo-Optical Instrumentation Engineers (SPIE) Conference Series. p. 1, doi:10.1117/12.856798
- Van Cleve J. E., et al., 2010, in American Astronomical Society Meeting Abstracts. p. 420.02
- Vida K., Kovári Z., Švanda M., Oláh K., Strassmeier K. G., Bartus J., 2007, *Astronomische Nachrichten*, **328**, 1078
- Weber M., Strassmeier K. G., Washuettl A., 2005, *Astronomische Nachrichten*, **326**, 287
- van Saders J. L., Pinsonneault M. H., 2013, *ApJ*, **776**, 67

APPENDIX A: FIGURES

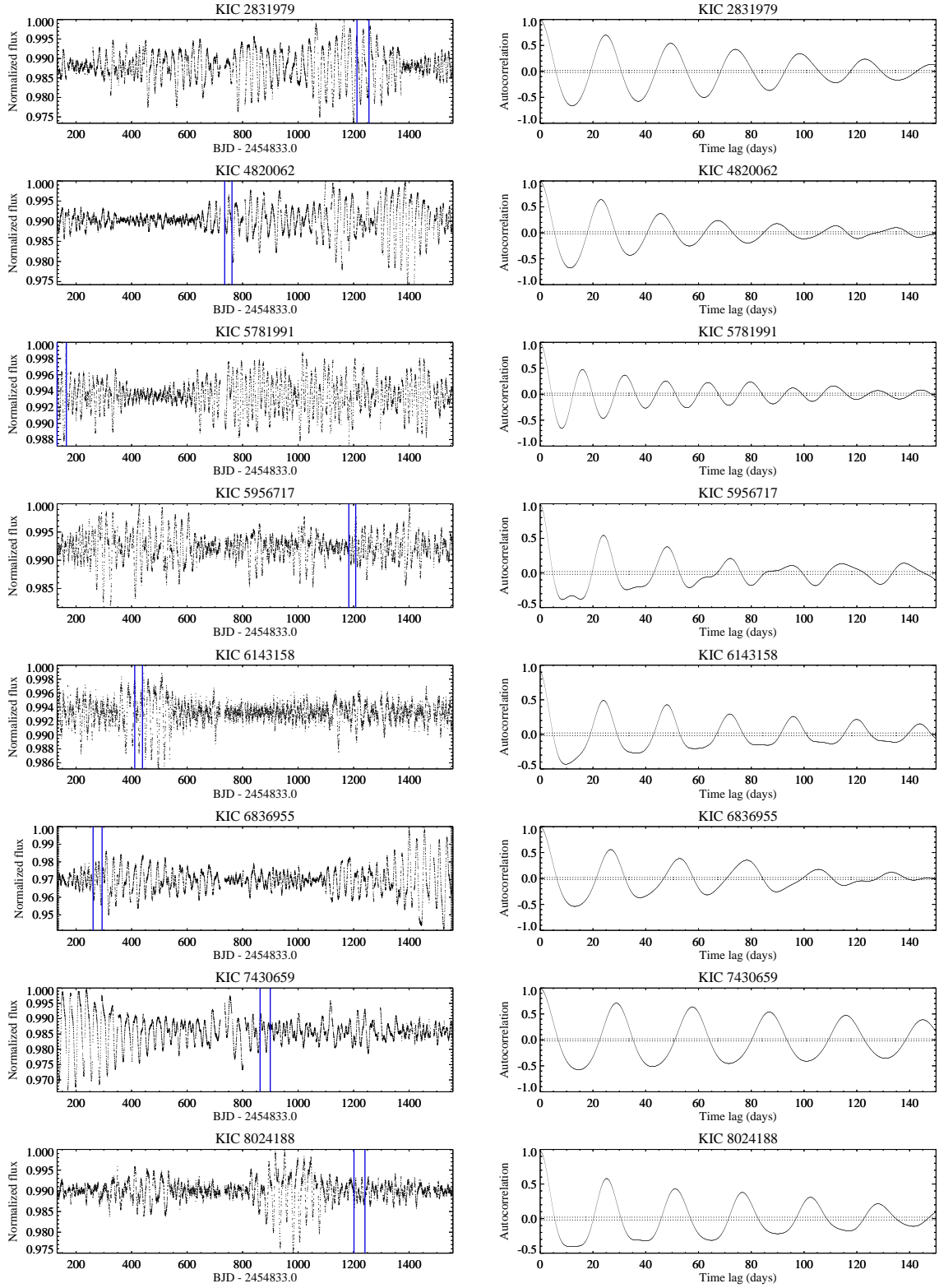


Figure A1. Left: Photometric times series of *Kepler* stars (from top to bottom) KIC 2831979, KIC 4820062, KIC 5781991, KIC 5956717, KIC 6143158, KIC 6836955, KIC 7430659, KIC 8024188, KIC 8037792, KIC 8495770, KIC 9996105, KIC 10079452, KIC 10279927, KIC 10460082, KIC 10514649, KIC 11199277 and KIC 12520213. The flux has been normalized to the maximum value observed along each time series. The vertical solid lines (in blue) display the initial and final times of the intervals considered for MCMC analysis (see Table 1). Right: Autocorrelation functions of the LCs of the stars in our sample. The dotted lines indicate the interval corresponding to $\pm\sigma$, where σ is one standard deviation of the autocorrelation as expected for a pure random noise with some degree of autocorrelation according to the large-lag approximation.

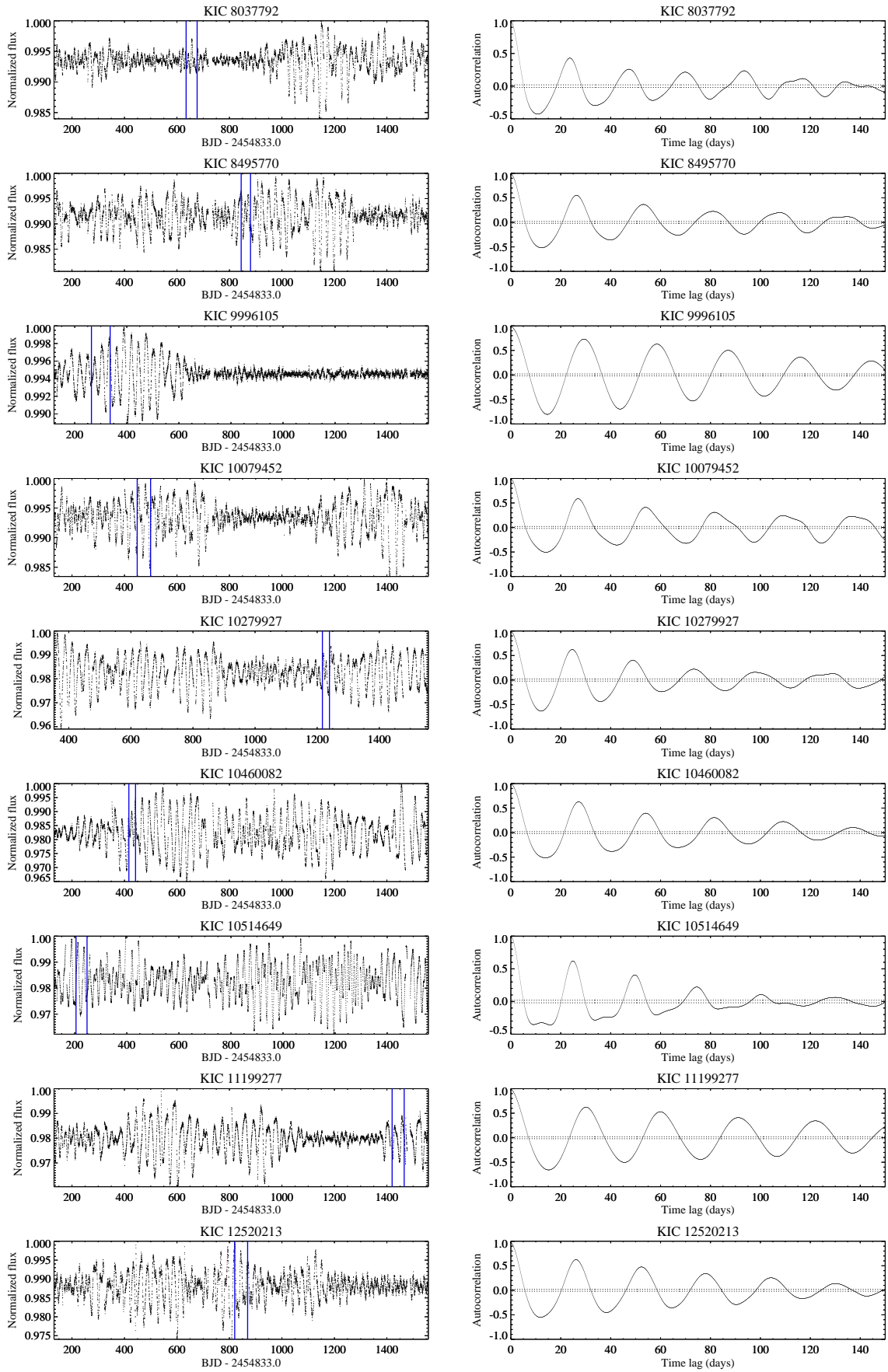


Figure A1. .continued.